

# Supplementary Notes

## Genetic Analyses Support the Contribution of mRNA $N^6$ -methyladenosine ( $m^6A$ ) Modification to Human Diseases Heritability

### Statistical model for $m^6A$ -QTL mapping

Unlike common omics data (e.g. ChIP-seq) that quantifies molecular trait by a single variable (e.g. read counts in a ChIP-seq peak),  $m^6A$ -seq experiments are characterized by a pair of input and immunoprecipitation (IP) measurements. To quantify  $m^6A$  level, we computed log fold enrichment of each peak by dividing the IP read counts by the input read count, each normalized by library sizes.

For a given testing window (as defined by joint  $m^6A$ -peaks), the read counts of IP (immunoprecipitated) and input (regular RNA-seq) in individual  $i$  are denoted as  $Y_i^{(1)}$  and  $Y_i^{(0)}$ , respectively. Let  $T_i^{(1)}$  and  $T_i^{(0)}$  be the library size of IP and input, respectively. We define log odds ratio (log-OR) as the  $m^6A$  quantitative phenotype:

$$\tilde{y}_i = \frac{Y_i^{(1)}/T_i^{(1)}}{Y_i^{(0)}/T_i^{(0)}} \quad (1)$$

**Correction for possible confounders:** Various factors (such as IP efficiency and GC content) may influence the measurement of  $m^6A$  level. Our strategy is to adjust the log-OR to account for covariates of peaks in sample-specific fashion.

We define observed log-OR of a peak  $j$  in sample  $i$  as:

$$\tilde{y}_{ij} = \frac{Y_{ij}^{(1)}/T_{ij}^{(1)}}{Y_{ij}^{(0)}/T_{ij}^{(0)}} \quad (2)$$

Learning how  $\tilde{y}_{ij}$  depends on IP efficiency and GC content in each sample would allow us to correct for deviation of  $\tilde{y}_{ij}$  due to those factors in a sample-specific manner.

**Adjusting for IP efficiency:** Variation of overall IP efficiency across individuals can have impact on the expected fraction of reads in IP. We adjust for this variation by estimating the difference of IP-efficiency between each sample  $i$  and the average across samples, using a strategy similar to WASP<sup>1</sup>. Let  $\bar{y}_{ij}$  be the average log-OR of peak  $j$  across all samples. We can plot  $\tilde{y}_{ij}$

vs.  $\bar{y}_j$  for all peaks in a sample  $j$  (**Figure SN 1a**). For samples with low IP efficiency, the lines would fall below diagonal line, and for samples with high IP efficiency, above the diagonal line. In order to capture the variation of IP efficiency across samples, we first fitted a quadratic function of  $\tilde{y}_{ij}$  against  $\bar{y}_j$  for each sample, as shown in (**Figure SN 1b**). Since the fitted curves are approximately linear, we then fitted a linear model for simplicity (**Figure SN 1c**). Let  $\hat{y}_{ij}$  be the expected log-OR for a given peak  $j$  in sample  $i$  (based on the fitted line), then our correction term for peak  $j$  in sample  $i$  is:

$$\Delta K_{ij} = \tilde{y}_{ij} - \bar{y}_j \quad (3)$$

**Adjusting for GC content:** Another technical covariate that has been shown to influence read count representation is GC content<sup>2,3</sup>. To adjust for the GC content bias, we group peaks of the same GC content into bins. Let  $b_{il}$  be the average log-OR of all peaks in bin  $l$  of sample  $i$ , and let  $b_{.l}$  be the average log-OR of all peaks in bin  $l$  over all samples. The difference of the two should reflect the GC effect. However, a sample may have higher log-OR across all peaks because of IP efficiency or other technical factors, so we should adjust for that. Let  $b_{i.}$  be the average log-OR of all peaks of sample  $i$ , and  $b_{..}$  be the average log-OR of all peaks of all samples. We define the deviation of bin  $l$  in sample  $i$  as:

$$F_{il} = (b_{il} - b_{.l}) - (b_{i.} - b_{..}) \quad (4)$$

As shown in **Figure SN 2**, the effect of GC content varies from sample to sample. We fitted a quadratic function of  $F_{il}$  vs. its GC content to get the correction term  $\Delta F_{il}$  for each peak given its GC content bin  $l$  in sample  $i$ .

Our log fold enrichment for sample  $i$  in peak  $j$  adjusting for IP efficiency and GC content is:

$$\tilde{y}_{ij} + \Delta K_{ij} + F_{il} \quad (5)$$

### **Re-analysis of ribosome-profiling data of METTL3 and YTHDF1 knockdown in Hela cells.**

To validate our finding of heterogeneous effect of m<sup>6</sup>A on downstream molecular traits, we used translation efficiency as an example and re-analyzed the ribosome profiling data of METTL3 (m<sup>6</sup>A methyltransferase) depleted Hela cells from reference<sup>4</sup>. The original paper focused on the target transcripts of YTHDF1 as defined by transcripts harboring YTHDF1-bound m<sup>6</sup>A peaks. To

systematically examine the effect of m<sup>6</sup>A depletion on translation efficiency, we first stratified all transcripts with m<sup>6</sup>A peaks and found the log<sub>2</sub> fold change of translation efficiency is slightly shifted towards up-regulation but still largely centered near 0 (**Extended Data Fig. 4c**). This result suggests that unlike targets of YTHDF1, which represent a translation promotion effect of m<sup>6</sup>A, more than half of m<sup>6</sup>A sites likely act as translation repressors while others act as translation activators. To understand this heterogeneous effect of m<sup>6</sup>A on translation efficiency, we stratified transcripts by RBP-bound m<sup>6</sup>A peaks (we defined targets by overlaps of RBP eCLIP-seq peak with m<sup>6</sup>A peaks in HeLa cells) and Welch's two-sample t-test was used to test the log<sub>2</sub> fold change in translation efficiency in RBP targets vs. non-targets, upon METTL3 knockdown. We reported 32 RBPs that showed significant difference of translation efficiency in targets vs. non-targets with FDR < 5%.

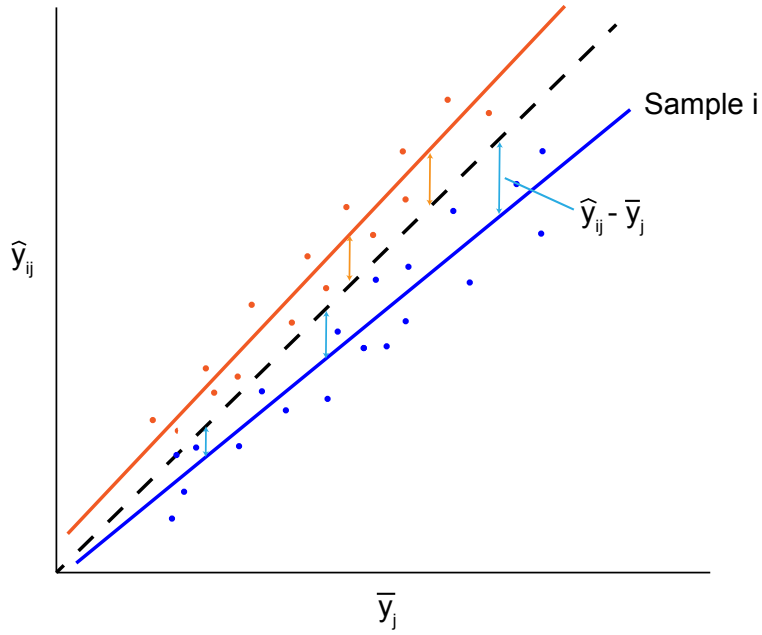
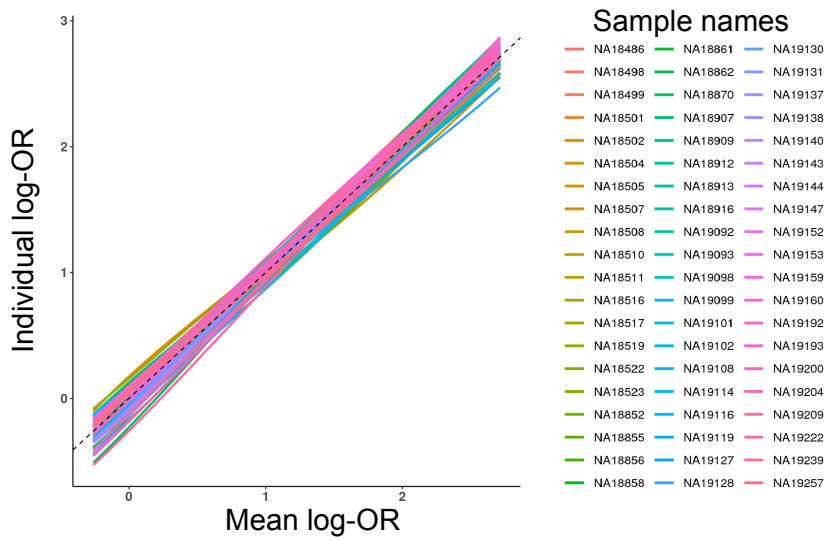
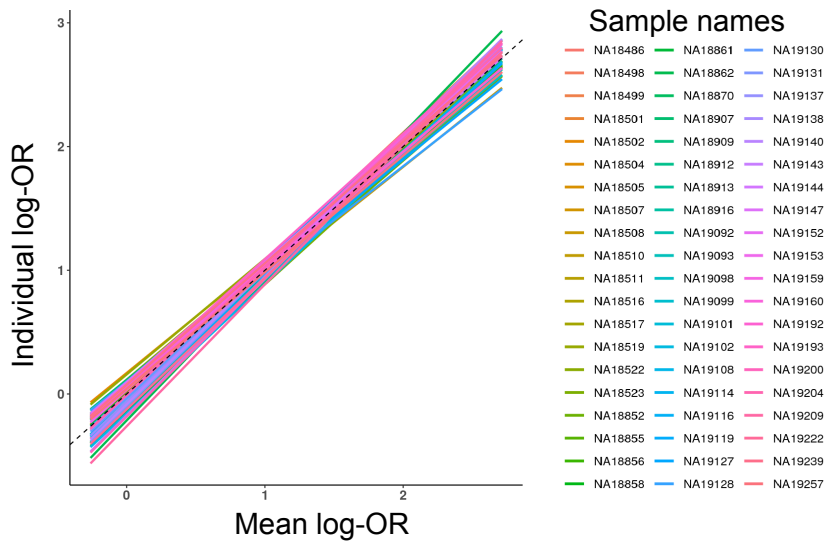
In order to further understand the heterogeneous effect of m<sup>6</sup>A on translation efficiency, we also re-analyzed the ribosome profiling data of YTHDF1 (m<sup>6</sup>A reader) depleted HeLa cells from reference<sup>4</sup>. We found the distribution of log<sub>2</sub> fold change of translation efficiency in all transcripts are shifted towards down-regulation (**Figure SN 3a**), which is due to improper normalization (**Figure SN 3b**). We normalized the libraries (**Figure SN 3c**) and examined the impact of YTHDF1 depletion on translation efficiency. Surprisingly, we found YTHDF1 knockdown led to overall reduction of translation efficiency in transcripts harboring YTHDF1-bound m<sup>6</sup>A sites, but there are 33% (proportion based on considering translation efficiency log<sub>2</sub> fold change < -0.5 or > 0.5 as having effects) YTHDF1 targets showing opposite effects (**Extended Data Fig. 4d**). This result suggests the effect of m<sup>6</sup>A on translation could be heterogeneous even in YTHDF1-targeted m<sup>6</sup>A sites, rather than previously thought simple translation promoting effects.

## Reference

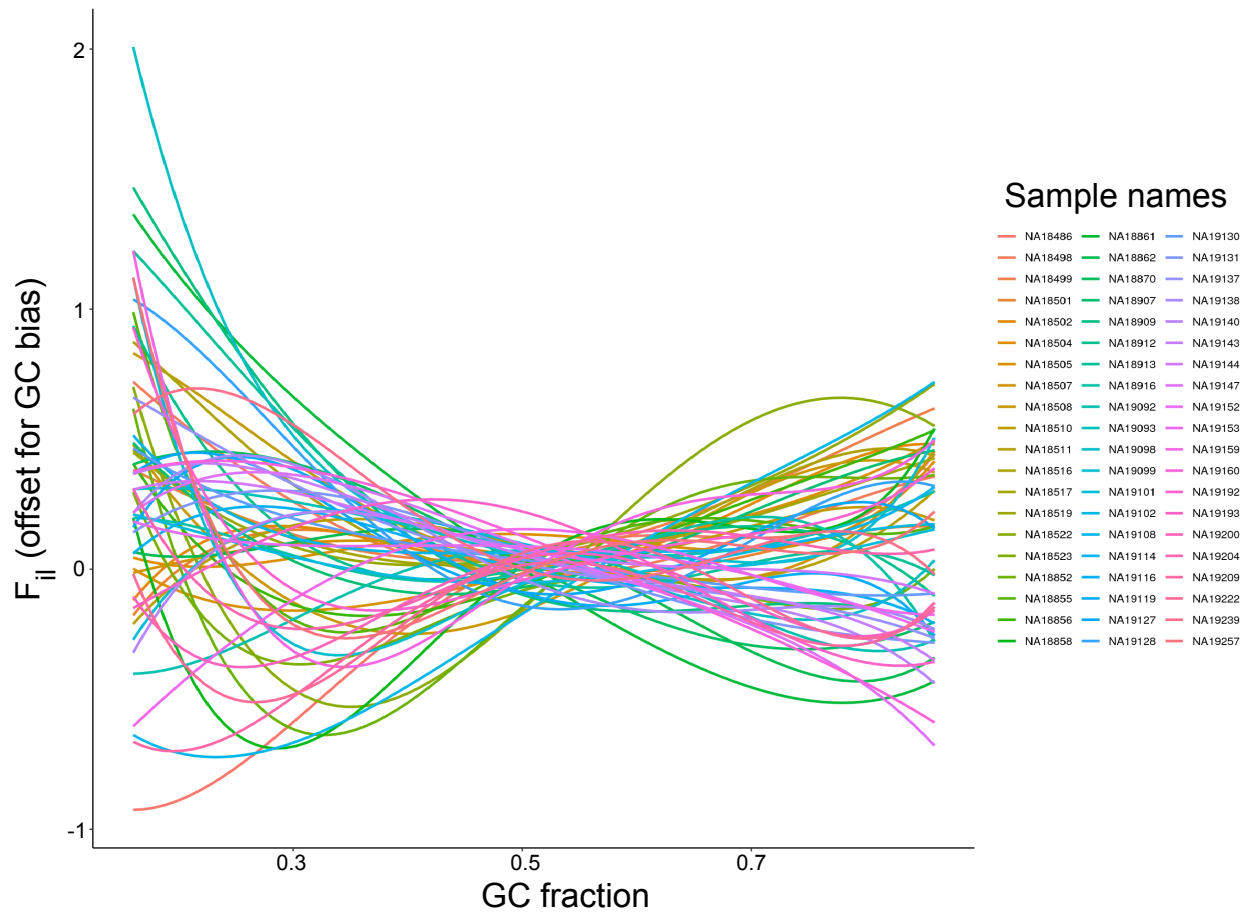
1. van de Geijn, B., McVicker, G., Gilad, Y. & Pritchard, J.K. WASP: allele-specific software for robust molecular quantitative trait locus discovery. *Nature methods* **12**, 1061-1063 (2015).
2. Kumasaka, N., Knights, A.J. & Gaffney, D.J. Fine-mapping cellular QTLs with RASQUAL and ATAC-seq. *Nat Genet* **48**, 206-13 (2016).
3. Stasinopoulos, D.M. & Rigby, R.A. Generalized Additive Models for Location Scale and

Shape (GAMLSS) in R. *Journal of Statistical Software; Vol 1, Issue 7 (2008)* (2007).

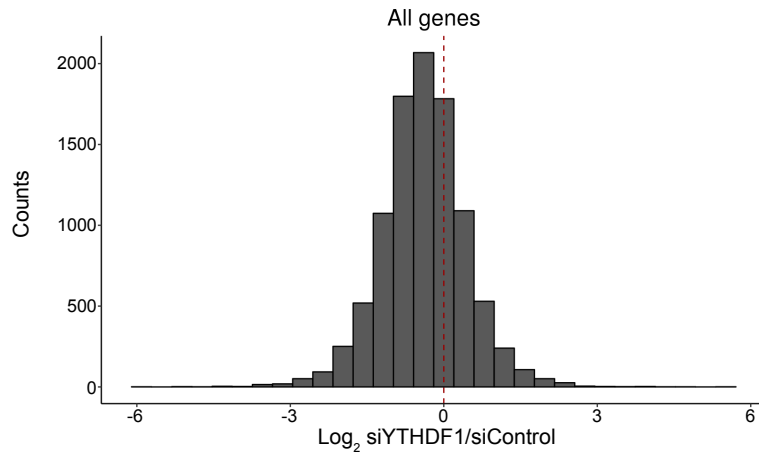
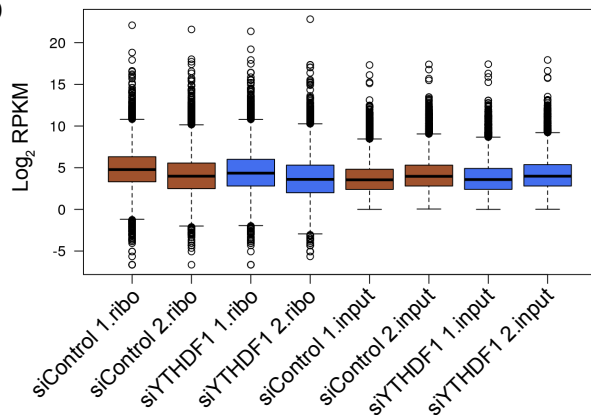
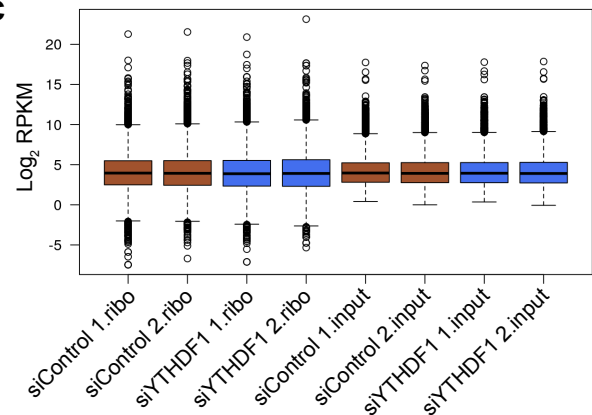
4. Wang, X. *et al.* N(6)-methyladenosine Modulates Messenger RNA Translation Efficiency. *Cell* **161**, 1388-1399 (2015).

**a****b****c**

**Figure SN 1: Fitting the overall IP efficiency correction term.** The fraction of reads coming from the peaks varies between experiments. We adjust for this variation by estimating the difference of IP-efficiency between each sample  $i$  and the average across samples as illustrated in panel **a**. We first fitted a quadratic function of individual log odds ratio vs. the mean log odds ratio across all samples as shown in panel **b**. Since the fitted curves are approximately linear, we simplified to fit the individual log odds ratio as a linear function of the mean log odds ratio across all samples as shown in panel **c**. All lines in panel **b** and **c** are fitted using  $n = 20044$  peaks.



**Figure SN 2: Fitting the GC bias correction term.** The GC content of a region can affect the sequencing depth of that region. This influence varies from sample to samples. To capture and correct for this GC bias, we fitted a correction term  $F_{ii}$  for each peak as a quadratic function of GC fraction of the peaks for each sample.

**a****b****c**

**Figure SN 3: Re-normalize ribosome profiling libraries.** We analyzed the ribosome profiling data from reference<sup>4</sup> and found the overall distribution of translation efficiency changes are shifted towards down-regulation as shown in panel a. We checked the distribution of read counts in individual samples of the analyzed data in the original paper as shown in b (n = 9,742 genes). The distribution of normalized read counts in each individual sample are shown in c (n = 9,742 genes). The lower and upper hinges correspond to the first and third quartiles. Horizontal line indicates median value, and whiskers correspond to the value no further than 1.5x inter-quartile range.